Journal of Glaciology, Vol. 37, No. 126, 1991

Length, width and slope influences on glacier surging

GARRY K. C. CLARKE
Department of Geophysics and Astronomy, University of British Columbia, Vancouver, British Columbia V6T 1W5, Canada

ABSTRACT. Statistical analysis of 1754 normal and surge-type glaciers of the Yukon Territory, Canada, reveals that the two glacier types have significantly different average geometries. Surge-type glaciers tend to be longer, wider and to have lower overall slope than normal glaciers. Because there are strong intercorrelations involving length, width and slope, it is not immediately clear which relationships are fundamental and which are secondary. Multiple correlation analysis allows these confusions to be resolved and reveals that the correlation between length and surge tendency is the fundamental one. The direct correlation between surge tendency and width and the inverse correlation between surge tendency and slope are entirely a result of the length–width and length–slope correlations. This conclusion may have implications for the glacier-surge mechanism because one prediction of the Kamb theory of surging is that small slopes (as opposed to great lengths) favour surging. Fowler's theory of surging predicts that glaciers for which the product θw^2 (where θ is slope and w is width) is small are more likely to be surge-type than those for which the product is large, but analysis of the correlation between this parameter and surge tendency lends no support to this claim.

INTRODUCTION

The Kamb (1987) and the Fowler (1987, 1989) theories of glacier surging lead to predictions that certain glacier geometries are conducive to surging. In outline, the Kamb theory proposes that surges are triggered by the transition from a localized subglacial water system to a distributed network of linked cavities and that this transition can occur when a dimensionless stability parameter Ξ falls below some critical value Ξ^*. For a step cavity Ξ takes the form

$$\Xi = 2^{\frac{1}{3}} \frac{(\theta\Lambda/\tau)^{\frac{3}{2}}}{D_0 M} \left(\frac{\eta}{\pi v p'}\right)^{\frac{1}{2}} h^{\frac{7}{6}} \qquad (1)$$

where θ is the longitudinal hydraulic gradient (assumed to equal surface slope), Λ is the "head gradient concentration factor", τ is the average tortuosity, $D_0 = 31\,\mathrm{km}$ is a natural length scale, M is the Manning roughness, η is the ice viscosity, v is the ice sliding velocity, p' is the effective pressure and h is the cavity step height. Of particular interest is the appearance of the surface slope θ in the numerator of the stability parameter; assuming all other influences are held constant, this implies that low slope is conducive to surging. The Fowler theory models a surge-type glacier as a spatially varying relaxation oscillator and is more abstract than the Kamb theory in its description of physical processes. Fowler (1989) introduced a surging criterion which may be expressed as $\omega < \omega^*$, where

$$\omega = \theta w^{\beta} \qquad (2)$$

and ω^* is some critical value of ω that distinguishes surging from non-surging glaciers. In the above expression θ is the mean bedrock slope, w is glacier width and $\beta \approx 2$. Since the mean surface slope and mean bed slope are approximately equal, I shall regard θ in Equation (2) as the surface slope.

Predictions of the Kamb and Fowler theories can be subjected to statistical testing by examining a large population of glaciers and determining whether surge-type (S-type) glaciers and normal (N-type) glaciers have significant geometric differences. The Canadian Glacier Inventory (CGI) of the Yukon Territory provides a suitable data set for testing this idea. A previous publication (Clarke and others, 1986) examined the length, elevation and slope influences on surging as well as the non-random geographical distribution of surge-type glaciers. One of the major conclusions claimed in Clarke and others (1986) is that long glaciers have a high probability of being surge-type and short glaciers have a high probability of being normal. Because length and slope for both N- and S-type glaciers have a strong inverse correlation, there is some confusion about whether length and slope correlations with surging are independent or whether the primary correlation with length (or slope) and the sec-

ondary correlation with slope (or length) are entirely a consequence of the length–slope correlation. A similar concern arises if width and ice thickness are added to the scheme. Large glaciers tend to be thick, wide and long, having low surface slope; small glaciers tend to be thin, narrow and short having high surface slope. Thus the problem of correlations between observational variables such as length l, width w, surface slope θ and thickness d are inescapable.

Kamb (1987, p. 9099) has used this ambiguity to claim that our CGI analysis supports the prediction of his theory that slope influences surging:

> "Despite these difficulties, a test of the ability of the linked cavity model to distinguish predictively in a statistical way between surge-type and nonsurge-type glaciers is provided by the observed correlation between glacier length and probability of surging in a large sample of Yukon glaciers [*Clarke et al.*, 1986, Figure 2*b*]. Glacier length does not directly enter as a parameter of the model, but since there is a strong inverse correlation between length and surface slope in the sample studied [*Clarke et al.*, 1986, Figure 4*a*], the observed correlation can be considered an inverse correlation between surge probability and slope θ, which is a parameter in the model. *Clarke et al.* [1986] concluded that the correlation was really with length alone and the slope had no effect, but a compelling statistical argument that required this conclusion was not given."

Fowler (1989, p. 261) echoed this concern and called for a statistical test of the ω stability parameter defined in Equation (2):

> "Their conclusion was that surging behavior correlated with length but not (independently) with surface slope. However, since long glaciers are also less steep, this could equally well be interpreted as meaning that gently-sloping glaciers tend to surge .... Clarke et al. did not report the widths of the glaciers in their data set. It would be interesting to test for the validity of a criterion such as (4.8) [equation (2) above], which involves purely geometrical criteria."

The aims of this paper are to seek correlations between surge tendency, length, width and slope and to test whether the observed correlations lend support to the predictions of the Kamb and Fowler theories.

DATA

The objective of the CGI is to complete an inventory of all glaciers in Canada as well as an inventory of glacier-related features such as glacierets, remnant glaciers, névés, snow patches, rock glaciers and pro-talus ramparts. Each glacier entry includes geographical coordinates, assorted geometrical data, and qualitative information on special features of the glacier. A complete description of formats and procedures is presented in Ommanney and others (1973), and further information is given in Ommanney (1980). The Yukon Territory component of the CGI was accomplished by a single investigator, Mr S. G. Collins, working for a period of 5 years. Research materials used by Collins include all available Canadian Government aerial photographs taken prior to 1965, a limited quantity of post-1965 vertical photographs, oblique aerial photographs from private sources, together with published and unpublished maps, scientific reports and mountaineering accounts. The Yukon Territory inventory contains a total of 4675 glaciers and glacier-related features. A purge of 2207 non-glacier features and 112 other unacceptable entries reduces the data set to 2356 glaciers. Not all glaciers are suitable for the present analysis. Several entries lack complete length or elevation information and when these have been removed the data set is reduced to 1984 entries. Clarke and others (1986) showed that tributary glaciers had a higher probability of being S-type than trunk glaciers. The likely explanation is that a surge occurring in a trunk glacier can induce surges of its tributary glaciers whereas the reverse situation is unusual. A further complication associated with tributary glaciers is that their lengths and slopes are measured as if they are themselves complete glaciers. For example, the length of a tributary glacier is taken as the distance from the farthest upflow point in the accumulation zone to the point at which the tributary joins the trunk glacier; unlike the trunk, the tributary has no proper terminus. Elimination of tributary glaciers further reduces the included data set. The final glaciers that are excluded from consideration are those that, for whatever reason, were recorded in the CGI as having no accumulation zone or no ablation zone. Culled in this way, the remaining glacier population is $N = 1754$.

The CGI glacier data that form the basis of this paper are the maximum length l, the mean width w of the main stream, the highest glacier elevation Z_{H} and the lowest glacier elevation Z_{L}. Of these measurements, the least clearly defined, and presumably the most vulnerable to subjective influences, is the determination of glacier width. Mean glacier slope is not tabulated in the CGI but can be calculated using the relation $\theta = \arctan[(Z_{\mathrm{H}} - Z_{\mathrm{L}})/l]$ and is presented in degrees. Surge tendency is a qualitative attribute included in the CGI data set. The system adopted is to introduce an integer "surge index" i that varies from 0 (no features suggesting surging) to 5 (definite surge characteristics). Determination of i is largely based on examination of aerial photographs and, where possible, comparison of photographs taken in different years. Assignment of i to a particular glacier was entirely the responsibility of S. G. Collins; whatever misgivings one might have about quantifying the qualitative, there is good reason to expect that a uniform methodology was applied. Inclusion of the surge index in the CGI makes it possible to seek correlations between surge tendency and glacier geometry. Table 1 shows a small sample of data extracted from the Yukon Territory data set; slope has been calculated from elevation data not presented in Table 1.

Figure 1 and Table 2 show the distribution of glaciers among the various i levels. Note the preponderance of glaciers in the $i = 0$ bin and the sparse distribution of glaciers in categories $i = 4$ and $i = 5$. At my request, S. G. Collins made post hoc estimates of the correspondence between i levels and the conditional probabilities $P(S = 1|i)$, i.e. the probability that a glacier having

https://doi.org/10.3189/S0022143000007255 Published online by Cambridge University Press

Table 1. *Sample of glaciers from the CGI data set*

Glacier	CGI identifer	Index i	Length km	Width km	Slope deg
Lowell	4*8ABG 001	5	74.5	4.5	2.44
Maxwell	4*8ABK 020	1	14.6	0.8	6.33
Tsirku	4*8BEA 001	4	17.5	1.7	3.66
Unnamed	4*9ACD 002	0	1.1	0.3	13.54
Kaskawulsh	4*9CAL 010	2	71.5	4.8	2.20
Unnamed	4*9CAN 056	3	5.4	0.5	10.39
Trapridge	4*9CAS 093	5	4.5	0.9	11.92

surge-index value i is S-type. These conditional probabilities are included in Table 2 and one can note that the probability a glacier in the $i = 5$ category is S-type is estimated at 97.5% whereas for a glacier in the $i = 0$ category the probability is 0.5%. Examination of Table 2 leads to the conclusion that $i = 4$ and $i = 5$ glaciers have a strong likelihood of being S-type and the remaining i levels match to glaciers that are predominantly N-type.

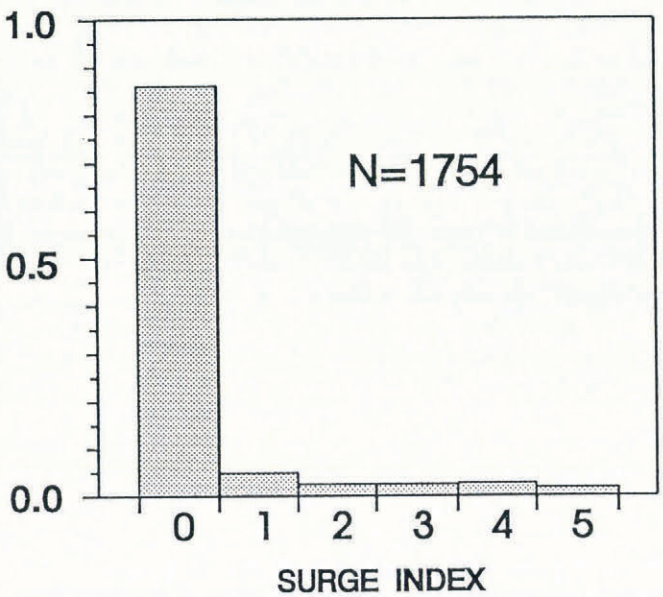

Fig. 1. Histogram showing distribution of surge-index values for 1754 glaciers in the Yukon Territory CGI data set. The vertical axis has been normalized so that the sum of the bar heights is unity.

Examination of histograms for l and w reveals that the length and width distributions tend to be log-normal. I therefore introduce the logarithmic transformations $L = \log_{10} l$ and $W = \log_{10} w$ to obtain variables that are approximately Gaussian-distributed (Fig. 2a and b). The presence of "empty bins" in histograms of Figure 2a and b is not a cause for concern. Visual smoothing shows that area missing from any of these bars is added to nearest neighbours and the overall result is approximately Gaussian. The explanation for these gaps is that length and width are recorded to the nearest 0.1 km; the logarithmic transformation produces empty bins unless the bar widths ΔL and ΔW are taken to be large. Slope-angle data require no transformation to yield a histogram that is approximately Gaussian (Fig. 2c). A histogram of $\Omega = \log_{10} \omega$, the logarithm of Fowler's parameter, is included for later reference (Fig. 2d). All of the foregoing histograms have been normalized to unit area and Gaussian curves of the form

$$f(x) = \frac{1}{\sigma\sqrt{2\pi}} \exp\left(-\frac{(x-\mu)^2}{2\sigma^2}\right) \qquad (3)$$

have been overplotted to illustrate the match between the two. In Equation (3) the variable x is intended to represent any one of L, W, θ or Ω where $\mu = E[x]$ is the mean value of x and $\sigma^2 = E[(x-\mu)^2]$ is the variance. (The notation $E[\cdot]$ indicates the expected value of the quantity within parentheses.) The mean and variance used in plotting the Gaussian curves in Figure 2a–c have been taken as the sample mean and sample variance calculated from the $N = 1754$ glaciers in the Yukon Ter-

Table 2. *Distribution of surge index i within Yukon Territory CGI data set*

Index i	Number n_i	Surge probability $P(S=1\|i)$	Surge characteristics
0	1510	0.005	No special features
1	85	0.020	Uncertain surge
2	42	0.030	Possible surge characteristics
3	42	0.200	Probable surge characteristics
4	46	0.800	Very probable surge characteristics
5	29	0.975	Certain surge characteristics
Totals	1754		

https://doi.org/10.3189/S0022143000007255 Published online by Cambridge University Press

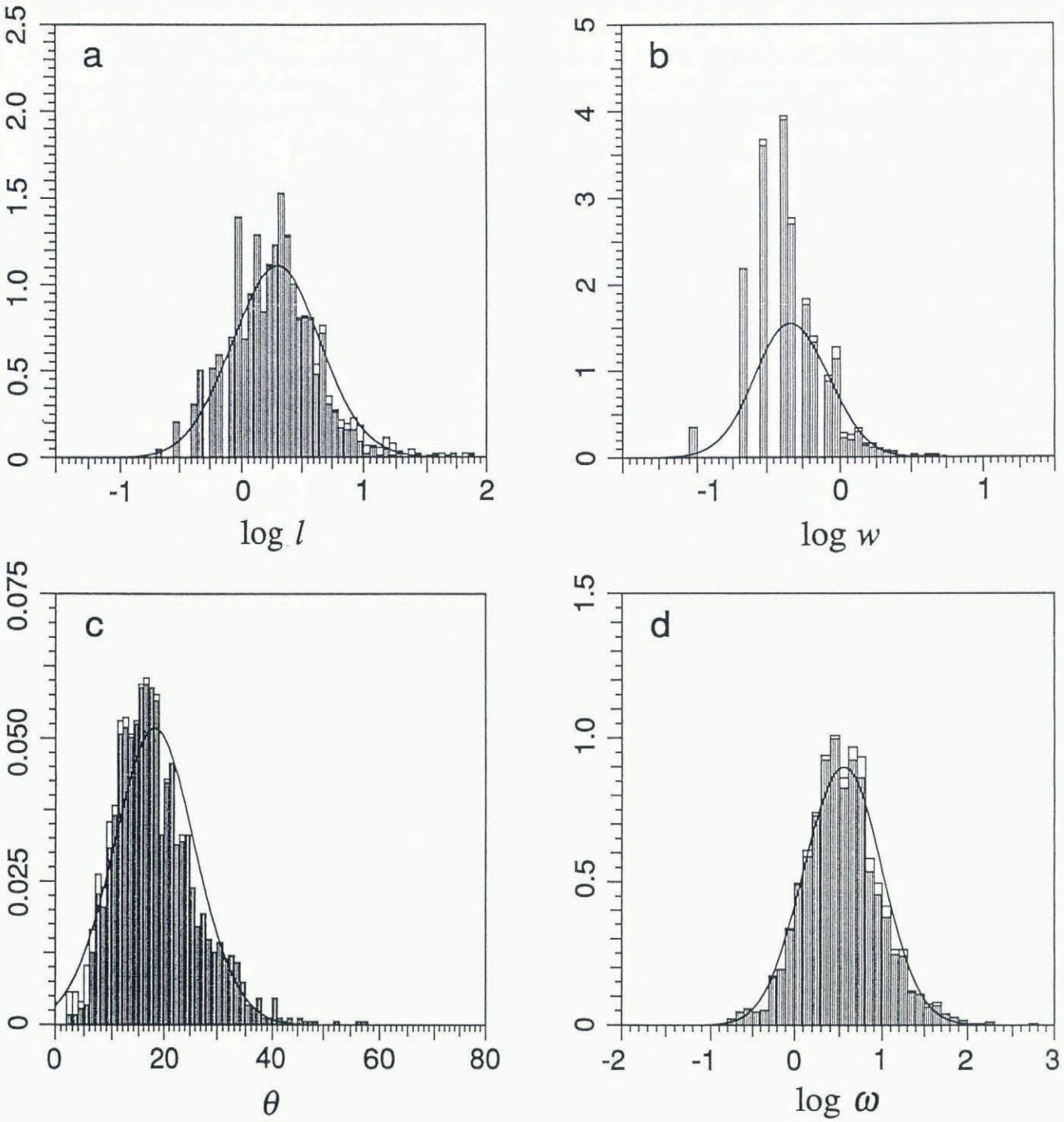

Fig. 2. Histograms calculated from the Yukon Territory CGI data set. These have been normalized to give unit area. Glaciers likely to be surge-type (those having surge index values of $i \geq 4$) are represented by the unshaded upper part of individual histogram bars. Gaussian curves having mean and variance values identical to the sample mean and sample variance have been superimposed. (a) Logarithmic length $L = \log_{10} l$. (b) Logarithmic width $W = \log_{10} w$. (c) Surface-slope angle θ. (d) Logarithm of Fowler's parameter $\Omega = \log_{10} \omega$.

ritory data set. Sample means are denoted by overlining and computed from

$$\overline{x} = \frac{1}{N} \sum_{n=1}^{N} x_n. \tag{4}$$

Sample variances are denoted by s^2 and computed from

$$s^2 = \frac{1}{N-1} \sum_{n=1}^{N} (x_n - \overline{x})^2. \tag{5}$$

In Equation (5), a denominator of N rather than $N-1$ leads to a biased estimate of the variance $\sigma^2 = E[(x - \mu)^2]$; thus Equation (5) is the preferred definition of sample variance.

In addition to the length, width and slope attributes it is necessary to incorporate the less precise attribute of "surge tendency". The simplest approach is to define a dichotomous variable S that takes the value $S = 0$ for normal glaciers and $S = 1$ for surge-type glaciers. Examination of Table 2 suggests that glaciers having surge

https://doi.org/10.3189/S0022143000007255 Published online by Cambridge University Press

index $4 \leq i \leq 5$ should be designated as type S and glaciers having $0 \leq i \leq 3$ should be designated type N. An alternative to this approach is to regard S as a measure of surge probability and adopt the definition

$$S = p(S = 1|i) \tag{6}$$

where $p(S = 1|i)$ is the probability that a glacier is surge-type given that its surge-index value is i. By performing the complete analysis presented in this paper using each of the two definitions, I have established that, although numbers differ, the results are insensitive to which approach is followed. Thus the probability-based definition of S defined in Equation (6) will be adopted.

CORRELATION ANALYSIS

The covariance between pairs of the attributes S, L, W and θ can be expressed in the general form

$$c_{jk} = \frac{1}{N-1}\sum_{n=1}^{N}(x_{jn} - \overline{x}_j)(x_{kn} - \overline{x}_k) \tag{7}$$

and these elements can be organized to form the covariance matrix **C**. Note that diagonal elements of **C** are simply the sample variances $s_j^2 = c_{jj}$. From the matrix elements c_{jk} the elements r_{jk} of the sample correlation matrix **R** can be formed using the relation

$$r_{jk} = \frac{c_{jk}}{\sqrt{c_{jj}c_{kk}}}. \tag{8}$$

These sample correlations are estimators of the correct (but unknown) population correlations ρ_{jk}.

Test of length, width and slope influences

The covariances between S, L, W and θ can be visually represented by scatter diagrams (Fig. 3a–f). In these diagrams a distinction between S- and N-type glaciers is indicated by assigning an × symbol to glaciers having $i = 4$ or $i = 5$ and a solid dot to all others. In the CGI, l and w are recorded to the nearest 0.1 km and the effects of this discretization are most apparent in Figure 3d. A problem with scatter diagrams involving discrete variables, and this is especially true of Figure 3a–c, is that substantial overplotting can occur making it impossible to distinguish whether a single plotted point represents one or many samples.

Information qualitatively expressed by scatter diagrams can be quantitatively summarized as a sample covariance or correlation matrix. Calculating these matrices for the attributes S, L, W and θ gives for the covariance matrix **C**:

$$\begin{array}{c} \\ S \\ L \\ W \\ \theta \end{array} \begin{array}{c} \begin{array}{cccc} S & L & W & \theta \end{array} \\ \begin{pmatrix} 0.03125 & 0.02956 & 0.01131 & -0.38587 \\ 0.02956 & 0.12905 & 0.04988 & -1.84820 \\ 0.01131 & 0.04988 & 0.06620 & -0.92601 \\ -0.38587 & -1.84820 & -0.92601 & 59.45316 \end{pmatrix} \end{array} \tag{9}$$

and for the correlation matrix **R**:

$$\begin{array}{c} \\ S \\ L \\ W \\ \theta \end{array} \begin{array}{c} \begin{array}{cccc} S & L & W & \theta \end{array} \\ \begin{pmatrix} 1.00000 & 0.46548 & 0.24875 & -0.28311 \\ 0.46548 & 1.00000 & 0.53967 & -0.66724 \\ 0.24875 & 0.53967 & 1.00000 & -0.46678 \\ -0.28311 & -0.66724 & -0.46678 & 1.00000 \end{pmatrix} \end{array}. \tag{10}$$

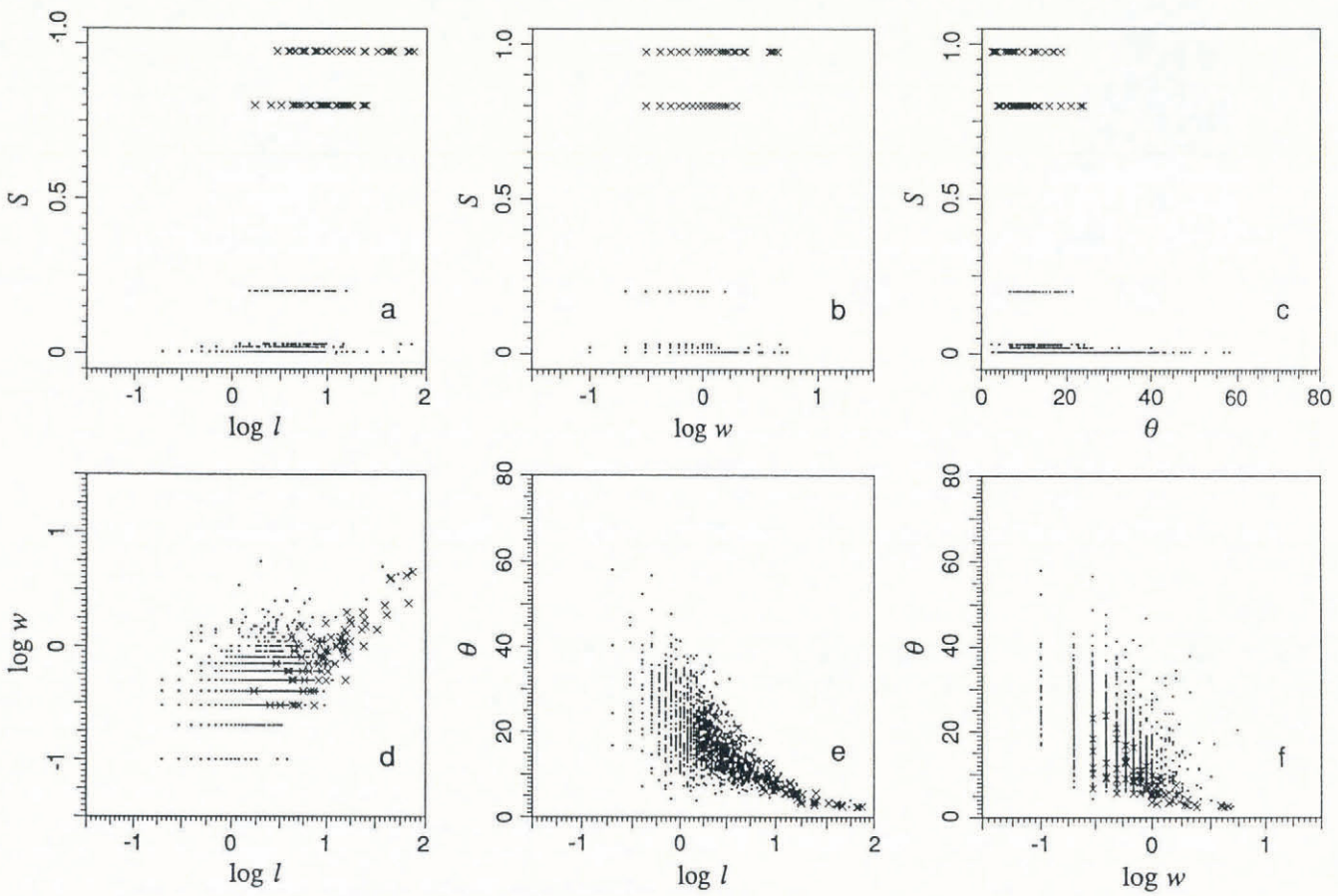

Fig. 3. Scatter diagrams for 1754 glaciers in the Yukon Territory CGI data set. (a) S vs L. (b) S vs W. (c) S vs θ. (d) L vs W. (e) L vs θ. (f) W vs θ.

https://doi.org/10.3189/S0022143000007255 Published online by Cambridge University Press

The null hypothesis, that off-diagonal terms of $\mathbf{R}$ vanish, can be tested using standard procedures and confidence intervals can be assigned to individual elements of the correlation matrix. To avoid burdening this section with technical discussion concerning significance testing, I shall simply state results and defer detailed discussion to a subsequent part of this paper. In matrix form, the 95% confidence limits for the off-diagonal terms of Expression (10) can be expressed as

$$\Delta\mathbf{R}_{0.95} = \begin{array}{c} \\ S \\ L \\ W \\ \theta \end{array} \begin{array}{c} \begin{array}{cccc} S & L & W & \theta \end{array} \\ \begin{pmatrix} 0.000 & 0.037 & 0.044 & 0.043 \\ 0.037 & 0.000 & 0.033 & 0.026 \\ 0.044 & 0.033 & 0.000 & 0.037 \\ 0.043 & 0.026 & 0.037 & 0.000 \end{pmatrix} \end{array}. \quad (11)$$

From Expression (11) it is apparent that the expected magnitude of error in the correlation estimates of Expression (10) is not large and would not alter the ranking of length and slope influences on surging. Close scrutiny of Expression (10) leads to the following conclusions:

1. Among L, W and θ, the attribute most strongly correlated with S is glacier length. Thus long glaciers tend to be surge-type.
2. The correlations of W and θ with S are of comparable magnitude and significantly less than that between L and S. The S–W correlation is direct (wide glaciers tend to be S-type) and the S–θ correlation is inverse (glaciers having low slope tend to be S-type).
3. The strongest correlation of all is the inverse correlation between L and θ. Long glaciers tend to have low slope. This raises the possibility that some component of the observed S–L correlation arises because of linkage from L to θ to S.
4. The correlation between L and W indicates that long glaciers tend to be wide.
5. The inverse correlation between W and θ indicates that wide glaciers tend to have low slope.

Sorting out the tangle of intercorrelations is the main difficulty in settling whether it is length or low slope that favours surging. The technique that allows the various possibilities to be analyzed is a standard method of multivariate statistics known as multiple-correlation analysis (e.g. Mardia and others, 1979, p. 170).

Applying the basic approach of multiple-correlation analysis to the problem of surging, one postulates the existence of a linear relationship of the form

$$Y = \sum_{m=1}^{M} \beta_m x_m \quad (12)$$

where β_m are constant coefficients and, for the present work, $M = 3$, $x_1 = L$, $x_2 = W$ and $x_3 = \theta$. The covariance between S and Y can be computed using Equation (7) and will differ according to the values assigned to β_m. Using the method of Lagrange multipliers (e.g. Lanczos, 1970, p. 43–48), values of β_m can be found that maximize the covariance c_{SY} subject to appropriate constraints (Morrison, 1990, p. 94–95). From this, a maximized value of the correlation r_{SY} can be calculated. This correlation is referred to as the multiple correlation between S and the remaining variables L, W and θ, and is denoted $r_{1\cdot 2\ldots M}$ in the general case and $r_{S\cdot LW\theta}$ for the present application. For the $M = 3$ case, the multiple correlation $r_{1\cdot 234}$ is evaluated by partitioning the correlation matrix into the following sub-matrices:

$$\mathbf{R}_{12} = \begin{pmatrix} r_{12} & r_{13} & r_{14} \end{pmatrix}, \quad (13)$$

$$\mathbf{R}_{21} = \begin{pmatrix} r_{12} \\ r_{13} \\ r_{14} \end{pmatrix}, \quad (14)$$

$$\mathbf{R}_{22} = \begin{pmatrix} r_{22} & r_{23} & r_{24} \\ r_{23} & r_{33} & r_{34} \\ r_{24} & r_{34} & r_{44} \end{pmatrix}, \quad (15)$$

and evaluating

$$r_{1\cdot 234} = \sqrt{\mathbf{R}_{12}\mathbf{R}_{22}{}^{-1}\mathbf{R}_{21}} \quad (16)$$

where $\mathbf{R}_{22}^{-1}$ denotes the matrix inverse of $\mathbf{R}_{22}$. Performing this evaluation for the matrix $\mathbf{R}$ gives $r_{S\cdot LW\theta} = 0.46695$ as the multiple-correlation coefficient. It is interesting to compare this value to those of the simple correlations appearing in Expression (10): specifically, $r_{SL} = 0.46548$ and $r_{S\theta} = -0.28311$. Because $r_{S\cdot LW\theta}$ and r_{SL} are essentially equal, one can immediately conclude that the primary correlation is between S and L and that virtually no part of the S–θ and S–W correlations is independent of the S–L correlation. The observed inverse correlation between S and θ therefore appears to have no fundamental importance. If the alternative possibility is tested, that the S–θ correlation is the crucial one, the argument runs as follows: the magnitude of the S–θ correlation is $|r_{S\theta}| = 0.28311$ whereas that of the multiple correlation $r_{S\cdot LW\theta} = 0.46695$. (The square root in Equation (16) removes all information concerning the algebraic sign.) Thus L and/or W must carry information concerning surge tendency. Two informative statistics are

$$J_{SL} = \frac{r_{S\cdot LW\theta} - r_{SL}}{r_{S\cdot LW\theta}}, \quad (17)$$

which represents the fraction of the multiple correlation $r_{S\cdot LW\theta}$ that is unexplained by the simple correlation r_{SL}, and

$$J_{S\theta} = \frac{r_{S\cdot LW\theta} - r_{S\theta}}{r_{S\cdot LW\theta}}, \quad (18)$$

which represents the fraction of the multiple correlation that is unexplained by the simple correlation $r_{S\theta}$. For the CGI Yukon Territory data set, sample values of Equations (17) and (18) are $J_{SL} = 0.00315$ and $J_{S\theta} = 0.39371$. If these sample values correctly represent the population statistics, then the following statements can be made: less than 0.32% of the multiple correlation between S and L, W and θ is unexplained by the correlation between S and L; less than 39.4% of the multiple correlation is unexplained by the correlation between S and θ. Equivalently, more than 99.68% of the multiple correlation is explained by the correlation between S and L; more than 60.6% of the multiple correlation is explained by the correlation between S and θ. To summarize, virtually all of the correlation between surge tendency and length, width and slope can be attributed to the correl-

https://doi.org/10.3189/S0022143000007255 Published online by Cambridge University Press

ation between surge tendency and length. In contrast, the Kamb theory would seem to predict that the (inverse) correlation between surge tendency and slope should be the predominant one. The statistical significance of these assertions is high, but this matter will be treated separately.

Test of influence of Fowler's parameter

My final task is to seek correlations between surge tendency and the Fowler parameter. This could be introduced as a fifth variable into the correlation matrix of Expression (10) but there is no reason to be interested in correlations between Ω and W or θ since Ω itself involves both of these quantities. Thus I simply consider the intercorrelations of S, L and Ω. For this analysis

$$\mathbf{C} = \begin{array}{c} \\ S \\ L \\ \Omega \end{array} \begin{array}{c} \begin{array}{ccc} S & L & \Omega \end{array} \\ \begin{pmatrix} 0.03125 & 0.02956 & 0.00854 \\ 0.02956 & 0.12905 & 0.04755 \\ 0.00854 & 0.04755 & 0.19713 \end{pmatrix} \end{array} \tag{19}$$

and

$$\mathbf{R} = \begin{array}{c} \\ S \\ L \\ \Omega \end{array} \begin{array}{c} \begin{array}{ccc} S & L & \Omega \end{array} \\ \begin{pmatrix} 1.00000 & 0.46548 & 0.10882 \\ 0.46548 & 1.00000 & 0.29811 \\ 0.10882 & 0.29811 & 1.00000 \end{pmatrix} \end{array}. \tag{20}$$

Multiple-correlation analysis of Equation (20) yields $r_{S\cdot L\Omega} = 0.46653$ compared to $r_{S\Omega} = 0.10882$ and $r_{SL} = 0.46548$. It is apparent that the correlation between surge tendency and the Fowler parameter is low and that, like slope, the Fowler parameter contributes negligibly to the multiple-correlation coefficient.

TESTS OF STATISTICAL SIGNIFICANCE

Questions of statistical significance cannot be left unaddressed, but the following section can be skipped by those who have no appetite for these matters.

Correlation estimates

Off-diagonal terms r_{jk} of the sample correlation matrix can be tested one at time against the null hypothesis that the true population correlation is $\rho_{jk} = 0$. (To reduce visual clutter, subscripts will henceforth be dropped from r and ρ except when they are essential for clarity.) For the case $\rho = 0$, the sampling distribution of r can be found from the statistic

$$t = r\sqrt{\frac{N-2}{1-r^2}}, \tag{21}$$

which has a Student t distribution with $N-2$ degrees of freedom. The criterion for rejecting the null hypothesis is

$$|t| > t_{\alpha/2;N-2} \tag{22}$$

where $t_{\alpha/2;N-2}$ is the upper 50α percentage point of the t distribution with $N-2$ degrees of freedom (e.g. Morrison, 1990, p. 102–03). For $N = 1754$, the order is essentially infinite and the t distribution approaches the unit normal-distribution. (A unit-normal distribution is a special case of Equation (3) obtained by setting $\mu = 0$ and $\sigma = 1$.) Assuming that $\alpha = 0.001$, standard statistical tables give $t_{0.0005;\infty} = 3.291$. Using Equation (21) to evaluate the matrix elements that correspond to those of the correlation matrix in Expression (10) leads to the conclusion that the null hypothesis can be rejected for all the correlations to a confidence level that far exceeds 99.9999%.

Confidence limits can also be placed on the estimated correlation coefficients r_{jk} of Expression (10). To obtain these, I used the standard procedure developed by Fisher (1921) and described in Morrison (1990, p. 101–06) and elsewhere. For each off-diagonal element of the correlation matrix, the sample correlation r has a non-Gaussian distribution about the true correlation ρ. The transformed variable

$$z = \frac{1}{2}\ln\left(\frac{1+r}{1-r}\right), \tag{23}$$

known as Fisher's z statistic, can be shown for large N to be normally distributed with mean value

$$\zeta = \frac{1}{2}\ln\left(\frac{1+\rho}{1-\rho}\right), \tag{24}$$

and variance

$$\mathrm{var}\,(z) = \frac{1}{N-3}. \tag{25}$$

It is therefore a simple matter to perform significance tests on z and then, by performing the reverse transformation

$$r = \frac{\exp(2z)-1}{\exp(2z)+1} = \tanh z, \tag{26}$$

obtain corresponding values of r. Following this approach, the probability that the sample correlation r lies within a given range can be evaluated using the relation

$$\tanh\left(z - \frac{z_{\alpha/2}}{\sqrt{N-3}}\right) \le \rho \le \tanh\left(z + \frac{z_{\alpha/2}}{\sqrt{N-3}}\right) \tag{27}$$

where tanh is a hyperbolic tangent and $z_{\alpha/2}$ is the upper 100α percentage point of the unit-normal distribution (e.g. Morrison, 1990, p. 8–9). Applying Inequality (27) to off-diagonal elements, the correlation matrix of Expression (10) yields estimates of the error magnitudes for the individual matrix elements. This procedure has been followed to obtain the error estimates given in Expression (11). Because the statistic z as defined in Equation (23) is normally distributed, it follows that the sampling distribution of any correlation coefficient r_{jk} has the form

$$f(r) = \frac{1}{(1-r^2)\sqrt{2\pi(N-3)}}\exp\left[-\frac{[z(r)-\zeta]^2}{2(N-3)}\right], \tag{28}$$

a fact that will be used in subsequent Monte Carlo simulations.

Multiple-correlation estimates

Confidence limits can be placed on estimates of the multiple-correlation coefficient once the sampling distribution of $r_{S\cdot LW\theta}$ has been determined. The sampling distribution for multiple-correlation coefficients was first

https://doi.org/10.3189/S0022143000007255 Published online by Cambridge University Press

found by Fisher (1928) who showed that for r^2 the distribution was

$$f^*(r^2) = \frac{(1-r^2)^{(N-p-1)/2}(1-\rho^2)^{N/2}}{\Gamma[\frac{1}{2}(N-p+1)]\Gamma(\frac{1}{2}N)} \cdot \sum_{m=0}^{\infty} \frac{\rho^{2m}(r^2)^{\frac{1}{2}(p-1)+m-1}\Gamma^2(\frac{1}{2}N+m)}{\Gamma(m+1)\Gamma[\frac{1}{2}(p-1)+m]} \quad (29)$$

where the correlation matrix $\mathbf{R}$ is $p \times p$, $\Gamma(\cdot)$ is the gamma function (Press and others, 1986, p. 156–57), and N is the sample size. This important result is widely quoted in the literature on multivariate analysis (e.g. Anderson, 1958, p. 93–96). The sampling distribution of $|r|$ is found from Equation (29) using the fact that

$$f(r) = f^*(r^2)\,\mathrm{d}(r^2)/\mathrm{d}r = 2rf^*(r^2). \quad (30)$$

Numerical evaluation of Equation (29) presents several minor difficulties. The arguments of the gamma function can be large and the actual function values can far exceed the overflow limits of digital computers. It is therefore essential to evaluate each term of Equation (29) by logarithmic additions and subtractions rather than by multiplications and divisions. Both the numerator and denominator of terms in Equation (29) can be huge but the net result is not. A second cautionary point is that the summation at first diverges then converges and terms near $m = 0$ as well as those for $m \to \infty$ can be vanishingly small.

It might be asked if the error magnitude of individual elements of the matrix $\mathbf{R}$ can be large enough to alter the conclusion that width and slope are not independently correlated with surge tendency. The answer is not immediately apparent from separate examination of the confidence limits on estimates of r_{SL} (using Inequality (27)) and $r_{S\cdot LW\theta}$ (using evaluations of Equation (30)). The root of the difficulty is apparent from Figure 4. The sampling distributions for both r_{SL} and $r_{S\cdot LW\theta}$ appear roughly Gaussian. If both statistics were independent of each other, the difference between individual pairs $r_{S\cdot LW\theta}$ and r_{SL} could be as large as 0.10. This would occur if $r_{S\cdot LW\theta}$ lay at the high end of its range and r_{SL} at the low end. In fact, the two statistics are strongly correlated but it is not self-evident what the likely range of differences might be. I know of no statistical theory that treats this question and have therefore employed Monte Carlo methods to estimate the sampling distributions of the statistics J_{SL} and $J_{S\theta}$.

A naive and incorrect approach to this Monte Carlo simulation is to start with the assumption that the correlation matrix $\mathbf{R}$ as given in Expression (10) correctly describes the population correlations and then use Equation (28) to introduce random perturbations to off-diagonal elements of Expression (10). The problem with this thinking is that it ignores the fact that off-diagonal elements of $\mathbf{R}$ are mutually correlated and a perturbation in any one element should affect all others. A correct procedure that respects the influence of these intercorrelations is outlined below.

I begin by assuming that the covariance matrix of Expression (9) correctly describes the population values of c_{jk}. Correlation matrices are necessarily symmetric and, by standard methods of linear algebra (e.g. Strang, 1980, p. 190–95), such matrices can be diagonalized by a rotational transformation $\mathbf{V}^T\mathbf{C}\mathbf{V} = \mathbf{D}$, where $\mathbf{V}$ and $\mathbf{V}^T$ are respectively the transformation matrix and its transpose. To determine $\mathbf{V}$ and $\mathbf{D}$, I employed the Jacobi method described in Press and others (1986, p. 342–49). Once rotated to diagonal form, the diagonal elements correspond to sample variances of some

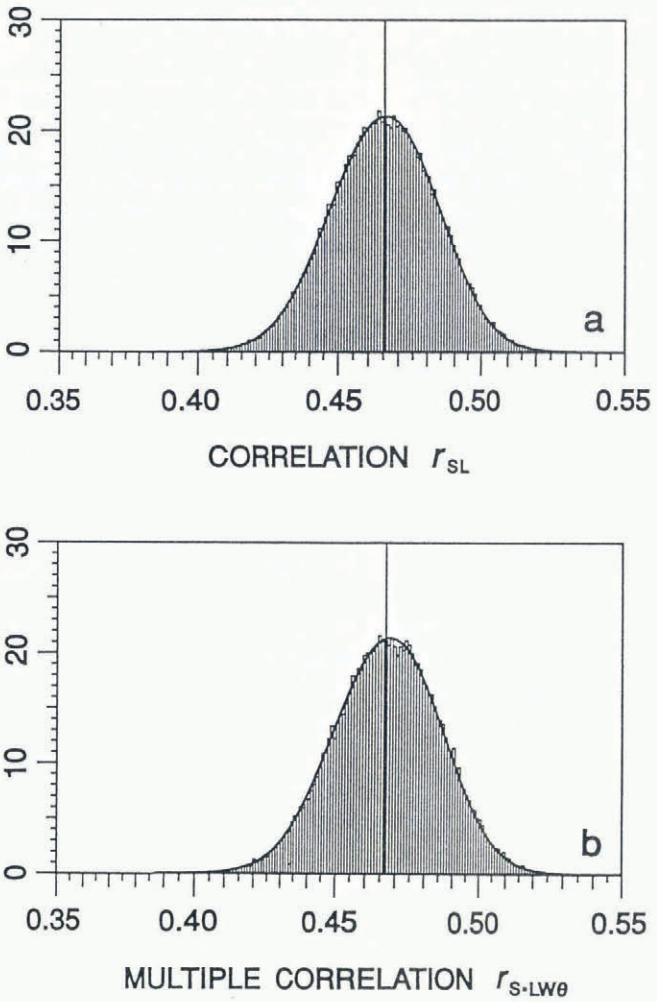

Fig. 4. Results of Monte Carlo simulation to estimate the sampling distribution of simple- and multiple-correlation coefficients. It is assumed that the correlation matrix for the infinite population is identical to that given by Expression (10) and that the size of individual samples drawn from this population is $N = 1754$. The number of Monte Carlo simulations used to estimate the sampling distributions is 100 000. Population values of the simple- and multiple-correlation coefficients are indicated by a vertical line. The solid curves are theoretical sampling distributions and confirm that the Monte Carlo estimates closely approximate the correct distributions. (a) Comparison of theoretical and simulated distributions of r_{SL} about the assumed population value of $\rho_{SL} = 0.46548$. (b) Comparison of theoretical and simulated distributions of $r_{S\cdot LW\theta}$ about assumed population value $\rho_{S\cdot LW\theta} = 0.46695$.

https://doi.org/10.3189/S0022143000007255 Published online by Cambridge University Press

new set of variables $u_1 = v_{11}S + v_{12}L + v_{13}W + v_{14}\theta$, $u_2 = v_{21}S + v_{22}L + v_{23}W + v_{24}\theta$, etc. These are obviously *not* directly observed quantities but they can be treated as such. The diagonal elements d_{11}, d_{22}, d_{33} and d_{44} of $\mathbf{D}$ are simply the respective sample variances s_1^2, s_2^2, s_3^2 and s_4^2 of the derived variables u_1, u_2, u_3 and u_4. These variances are evaluated with respect to the sample means $\overline{u_1}$, $\overline{u_2}$, $\overline{u_3}$, $\overline{u_4}$. Standard statistical theory predicts that, for random samples drawn from a normal population of size N having mean μ and variance σ^2, the distribution of sample variance s^2, about the true population value σ^2 will have the form

$$f(x) = \frac{1}{2^{(N-1)/2}\Gamma[(N-1)/2]} x^{(N-3)/2} \exp(-x/2) \quad (31)$$

where

$$x = (N-1)s^2/\sigma^2 \quad (32)$$

and $f(x)$ is a χ^2 distribution having $\nu = N - 1$ degrees of freedom. For large values of ν the variable $q = \sqrt{2x} - \sqrt{2\nu}$ can be shown to have a unit-normal distribution. By using a random number generator (Press and others, 1986, p. 200–03) to generate normally distributed random values for x, Equation (32) can be employed to produce correctly distributed random values for s and effect statistically correct perturbations to $\mathbf{D}$ to obtain the diagonal elements d'_{11}, d'_{22} and d'_{33} of the perturbed matrix $\mathbf{D}'$.

Off-diagonal elements of $\mathbf{D}$ vanish but off-diagonal elements of $\mathbf{D}'$ do not. These off-diagonal perturbations can be found by noting that the correlation matrix associated with the diagonalized covariance matrix is simply the identity matrix $\mathbf{I}$. Off-diagonal perturbations to this correlation matrix are governed by the sampling distribution described by Equation (28) with $\zeta = 0$. The corresponding off-diagonal perturbations to $\mathbf{D}$ can be found using Equation (8) to obtain the relation $d'_{jk} = r'_{jk}(d'_{jj}d'_{kk})^{1/2}$ where r'_{jk} represent perturbations to the off-diagonal elements of the diagonalized covariance matrix. Applying this approach to each of the diagonal elements of $\mathbf{D}$, it is easy to generate a series of matrices $\mathbf{D}'$ that approximate $\mathbf{D}$ but include random error. The matrix transformation $\mathbf{V}\mathbf{D}'\mathbf{V}^T = \mathbf{C}'$ yields a randomly perturbed covariance matrix from which a randomly perturbed correlation matrix $\mathbf{R}'$ can be formed. The resulting correlation matrix $\mathbf{R}'$ is then subjected to multiple correlation analysis and by repeating this procedure a large synthetic sample of r'_{SL}, $r'_{S\theta}$ and $r'_{S\text{-}LW\theta}$ estimates can be generated. Using this Monte Carlo procedure, I generated 100 000 random $\mathbf{R}'$ matrices from which the sampling distributions for various correlation statistics could be calculated. Each of these matrices simulates the effect of drawing $N = 1754$ glaciers from an infinite population and computing the sample-correlation matrix. As a computational check, I have compared the simulated distributions for r_{SL} and $r_{S\text{-}LW\theta}$ with those predicted by statistical theory and obtained excellent agreement (Fig. 4).

The simulated sampling distribution and cumulative distribution function for the J_{SL} and $J_{S\theta}$ statistics are given in Figure 5. The intention of Figure 5 is to show the sensitivity of sample values of the J statistic to correctly distributed random error in the correlation matrix. As mentioned, these sampling distributions have been calculated by making the a priori assumption that the population values of $\mathbf{R}$ are known and correspond to Expression (10), but in reality $\mathbf{R}$ in Expression (10) is a sample from some population having unknown correlation attributes. For this reason, Figure 5 cannot be used as the starting point for significance testing of the J statistics for the CGI sample. Nevertheless, we can see that the sampling distribution of J_{SL} about the assumed population mean (Fig. 5a) suggests that sample values are likely to be within 1–2% per cent of the population

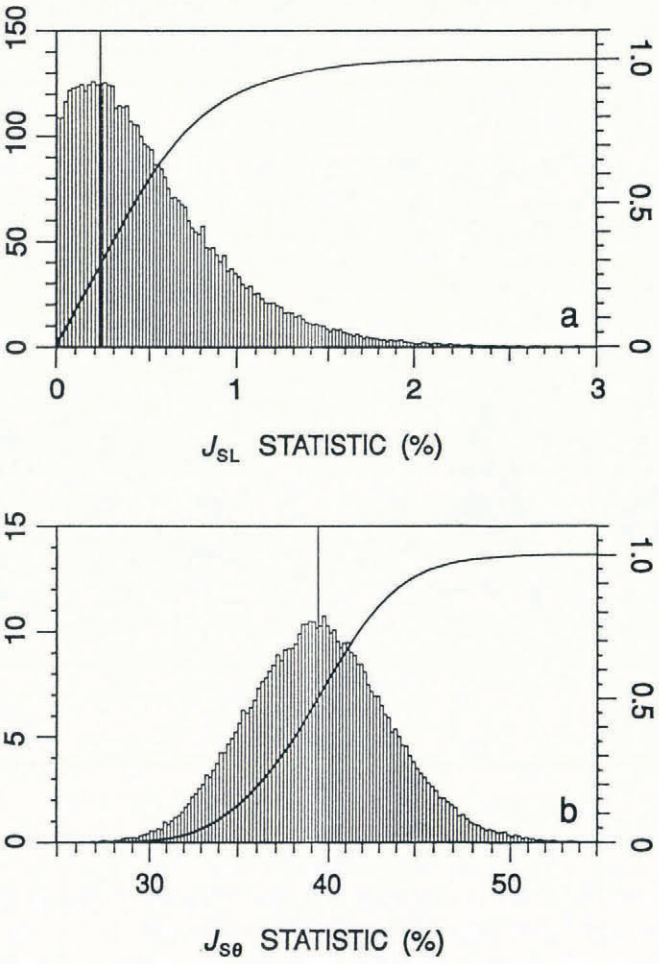

Fig. 5. Results of Monte Carlo simulation to estimate the sampling distribution of the J statistics for the correlations S–L and S–θ. It is assumed that the correlation matrix for the infinite population is identical to that of Expression (10) and that the size of individual samples drawn from this population is $N = 1754$. The number of Monte Carlo simulations used to estimate the sampling distributions is 100 000. The lefthand ordinate measures the amplitude of the probability density function for the J statistic. The righthand ordinate is the amplitude of the cumulative function (solid line) obtained by integrating the density function for the J statistic. The assumed population value for the J statistic is indicated by a vertical line. (a) Sampling distribution of J_{SL}. (b) Sampling distribution of $J_{S\theta}$.

https://doi.org/10.3189/S0022143000007255 Published online by Cambridge University Press

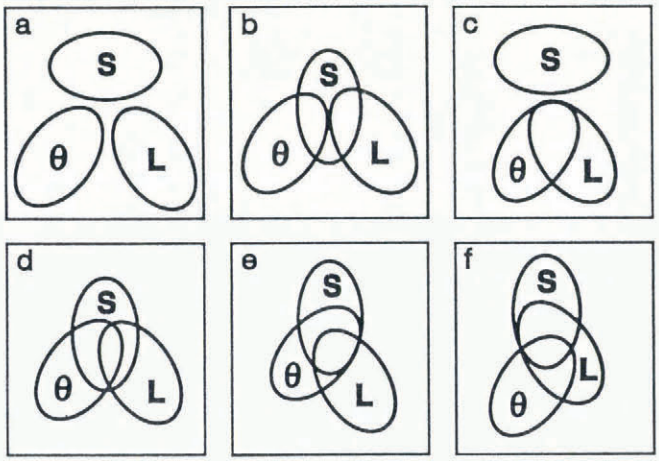

Fig. 6. Venn diagrams illustrating several possible correlation relationships between surge tendency S, slope θ and logarithmic length L. (a) Surge tendency, slope and length are uncorrelated. (b) Slope and length are uncorrelated but both correlate with surge tendency. (c) Slope and length are correlated but neither correlate with surge tendency. (d) Slope and length are mutually correlated and both correlate with surge tendency. The correlations between slope and surge tendency and length and surge tendency are not completely independent of each other but both have separate explanatory value. (e) Slope and length are mutually correlated and both correlate with surge tendency. All of the correlation between surge tendency and length can be explained in terms of the correlation between slope and length. Length has no explanatory value not already accounted for by the correlation between slope and surge tendency. (f) Slope and length are mutually correlated and both correlate with surge tendency. All of the correlation between surge tendency and slope can be explained in terms of the correlation between slope and length. Slope has no explanatory value not already accounted for by the correlation between length and surge tendency. This is the result of the present study.

value (indicated by a vertical line). Thus the conclusion that virtually all the multiple correlation $\rho_{S\cdot LW\theta}$ is explained by the simple correlation ρ_{SL} is not at risk. The sampling distribution for $J_{S\theta}$, on the other hand, is very broad (Fig. 5b) so the percentage discrepancy between sample values and the population value for this statistic is likely to be large. Fortunately, important conclusions do not hinge on this statistic.

CONCLUSIONS

Venn diagrams provide an efficient representation of the possible correlation relationships between length, slope and surge tendency. Several of these are summarized in Figure 6. Of particular interest are Figure 6d–f because they clarify the distinction I wish to make between the results of this study and other possibilities. For each of these cases, slope and length are mutually correlated and each correlates with surge tendency. In Figure 6d, slope and length each have explanatory value whereas in the remaining diagrams slope (Fig. 6e) or length (Fig. 6f) alone have explanatory value. The present analysis of the CGI Yukon Territory data set and that of Clarke and others (1986) points to the conclusion that the correlation between slope and surge tendency is that depicted in Figure 6f and that slope has no explanatory value.

How are we to regard Kamb's prediction that low slope favours surging? For insight, let us apply the Kamb theory to the following artificial situation: a sample of n glaciers is selected from a population having statistics identical to those of the CGI Yukon Territory data set. These glaciers are chosen to have identical length but to have slopes that are randomly distributed about the sample mean. The Kamb theory would predict that glaciers having lower than average slope have a greater tendency to be S-type than those having a greater than average slope. The CGI correlation analysis would predict that slope yields no information concerning surge tendency. From this perspective, the results of this paper contradict predictions of the Kamb theory. From a more generous perspective, the Kamb theory is a *local* theory of subglacial hydrology and necessarily employs local physical variables such as slope, effective pressure and step-cavity height. In contrast, length is a *global* variable which could not appear in a local theory, so no purely local theory would be capable of predicting a length influence.

With the Fowler prediction the situation is clearer. The prediction fails. None of the variables I have considered had a lower correlation with surge tendency than the parameter Ω. In fairness, the predicted correlation between S and Ω seems incidental to the main structure of Fowler's theory.

ACKNOWLEDGEMENTS

This research was supported by grants from the Natural Sciences and Engineering Research Council of Canada. I thank S. Ommanney and S. Collins for their huge contributions to the Canadian Glacier Inventory effort. Without this foundation to work from, the present project would have been inconceivable.

REFERENCES

Anderson, T. W. 1958. *An introduction to multivariate statistical analysis*. New York, John Wiley.

Clarke, G. K. C., J. P. Schmok, C. S. L. Ommanney and S. G. Collins. 1986. Characteristics of surge-type glaciers. *J. Geophys. Res.*, **91**(B7), 7165–7180.

Fisher, R. A. 1921. On the 'probable error' of a coefficient of correlation deduced from a small sample. *Metron*, **1**(4), 3–32.

Fisher, R. A. 1928. The general sampling distribution of the multiple correlation coefficient. *Proc. R. Soc. London, Sec. A*, **121**, 654–673.

Fowler, A. C. 1987. A theory of glacier surges. *J. Geophys. Res.*, **92**(B9), 9111–9120.

Fowler, A. C. 1989. A mathematical analysis of glacier surges. *SIAM J. Appl. Math.*, **49**(1), 246–263.

Kamb, B. 1987. Glacier surge mechanism based on linked cavity configuration of the basal water conduit system. *J. Geophys. Res.*, **92**(B9), 9083–9100.

Lanczos, C. 1970. *The variational principles of mechanics. Fourth edition.* Toronto. University of Toronto Press.

Mardia, K. V., J. T. Kent and J. M. Bibby. 1979. *Multivariate analysis.* New York, Academic Press.

Morrison, D. F. 1990. *Multivariate statistical methods. Third edition.* New York, McGraw-Hill.

Ommanney, C. S. L. 1980. The inventory of Canadian glaciers: procedures, techniques, progress and applications. *International Association of Hydrological Sciences Publication* 126 (Riederalp Workshop 1978 —*World Glacier Inventory*), 35–44.

Ommanney, C. S. L., J. Clarkson and M. M. Strome. 1973. Information booklet for the inventory of Canadian glaciers. Ottawa, Environment Canada, Inland Waters Directorate. (Glacier Inventory Note 4.)

Press, W. H., B. P. Flannery, S. A. Teukolsky and W. T. Vetterling. 1986. *Numerical recipes: the art of scientific computing.* Cambridge, Cambridge University Press.

Strang, G. 1980. *Linear algebra and its applications. Second edition.* New York, Academic Press.

The accuracy of references in the text and in this list is the responsibility of the author, to whom queries should be addressed.

MS received 18 Febuary 1991 and in revised form 10 May 1991